Műszaki Tudományos Közlemények vol. 21. (2024) 36–47.
DOI: Hungarian: https://doi.org/10.33895/mtk-2024.21.06
English: https://doi.org/10.33894/mtk-2024.21.06

SIMULATION OF THE VECTOR CONTROLLED PMSYM DRIVE BASED ON SIMPLIFIED MODELING STRUCTURES

Mária IMECS,[1] János FERENCZ,[2] András KELEMEN[3]

[1] *Technical University of Cluj-Napoca, Doctoral School, Faculty of Electrical Engineering, Cluj-Napoca, Romania, Maria.Imecs@emd.utcluj.ro*

[2] *Technical University of Cluj-Napoca, Doctoral School, Faculty of Electrical Engineering, Cluj-Napoca, Romania, janos.ferencz.phd.project@gmail.com*

[3] *Sapientia EHungarian University of Transylvania, Faculty of Technical and Human Sciences, Department of Electrical Engineering, Târgu Mureș, Romania, kandras@ms.sapientia.ro*

Abstract

The paper presents the simulation results of the simplified static (St) and dynamic (Dy) simulation structures (SimS), with voltage (U) and frequency (f) input, all of them based on a simplified mathematical model (MaMo) of the PM synchronous machine (SyM) corresponding to the operation mode with stator current vector perpendicular to the PM flux (CVpPMF). These results are compared with those simulated with vectorial speed controlled (VC) SimS-s where the longitudinal armature reaction is cancelled by means of two-phase current controllers in two different conditions: when the motor is fed by sine-wave voltages, and when it is connected to a PWM-inverter. By means of simulation of the St- and Dy_SimS-s the motor parameter identification calculations are verified, while the compatibility of the MATLAB/Simulink® motor block with the applied MaMo, required for the implementation of the vector control, is also verified using the VC-Sim-s.

Keywords*: PM synchronous motor, vector control, mathematical modelling, simulation structures.*

1. Introduction

The permanent magnet (PM) synchronous type machines belong to the most commonly used electrical machines besides the asynchronous motors. These can have sinusoidal or trapezoidal flux distribution of the magnetic field (DMF) in the air gap. The classical synchronous machines (SyM) have sinusoidal distribution DMF and those with trapezoidal DMF are considered "synchronous type" motors like the brushless direct current machines (BLDC), the conventional stepper motors and the motors with pole number ratio (4/3, 3/4, 5/2, 5/3, etc) different from 1, where the stator and rotor pole-numbers are not equal. The PMSyM-s are widely used as motors in the domain of electrical drives and as generators for energy production in wind turbine systems. This paper deals with the PMSyM with sinusoidal DMF whose mathematical model (MaMo) is based on the Park-theory.

2. The mathematical model of the PM synchronous machines

In **Figure 1** is presented the schematic structure of a one pole pair ($z_p = 1$) PMSyM, where θ is the rotor position with respect to the d (real) axis of the reference frame fixed to the stator. This coincides with the a_s stator phase magnetizing direction and it is expressed as an electrical angle.

According to the general Park-theory the two-phase MaMo of the SyM-s with sinewave DMF is expressed in the reference frame fixed to the rotor.

The dθ–qθ axes of the coordinate system (CooSy) correspond to the symmetry axes of the PM rotor **[1, 2]**, thus the orientation of the reference frame can be named PM-field orientation.

2.1. The general dynamic mathematical model of the PM synchronous machines

The general equations of the PMSyM without damping circuits can be deduced from the

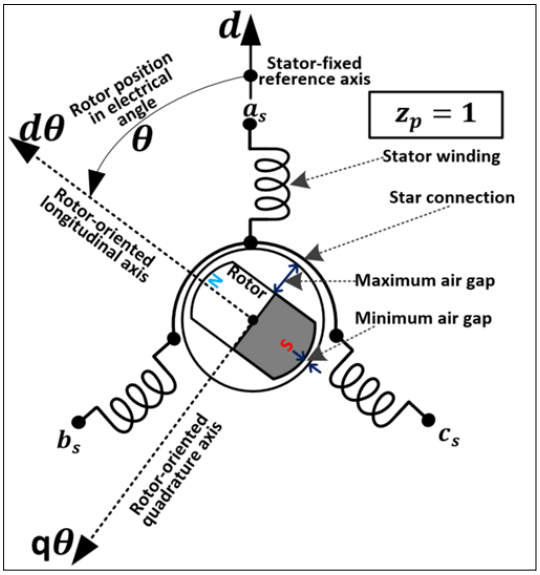

Fig. 1. *Structural principle diagram of the PMSyM with $z_p = 1$ pole pair.*

original Park-model by neglecting the rotor circuits and by replacing the magnetic flux of the exciting winding with the PM flux [3].

The voltage equation of the armature (stator) written with space phasors is

$$\underline{u}_{s\theta} = R_s \underline{i}_{s\theta} + \frac{d\underline{\Psi}_{s\theta}}{dt} + j\omega\underline{\Psi}_{s\theta}, \quad (1)$$

where $\underline{u}_{s\theta}$. $\underline{i}_{s\theta}$, and $\underline{\Psi}_{s\theta}$ are the space phasors of the armature voltage, current and armature flux, respectively, in rotor-oriented coordinate system, R_s is the stator resistance, ω is the electrical angular speed of the rotor

$$\omega = \frac{d\theta}{dt} \quad (2)$$

and θ is the angular position of the rotor as is shown in Figure 1 .

The armature resultant flux:

$$\underline{\Psi}_{s\theta} = \Psi_{PM} + \underline{\Psi}_{ss\theta}, \quad (3)$$

where Ψ_{PM} is the PM flux, the direction of which coincides with the real axis of the complex plane i.e. with the rotor-oriented dθ direct axis and $\underline{\Psi}_{ss\theta}$ is the armature reaction flux (ARF). This one can be written with the two-phase components (2PhCo) of the stator current as follows:

$$\underline{\Psi}_{ss\theta} = L_{sd} i_{sd\theta} + \mathrm{j} L_{sq} i_{sq\theta}, \quad (4)$$

where L_{sd} and L_{sq} are the longitudinal and quadrature three-phase inductances.

The dynamic torque in the motion equation is:

$$J_{Eq} \frac{d\omega_m}{dt} = m_e - m_L, \quad (5)$$

where J_{Eq} is the equivalent moment of inertia, ω_m the mechanical angular speed, m_e the electromagnetic torque (EMT) and m_L load torque.

The mechanical angular speed and the f_s frequency are proportional with the speed n measured in RPM („*revolution per minute*"). In the identification procedure of the motor parameters the below expressions are useful:

$$\omega_m = \frac{\omega}{z_p} = \frac{\pi n}{30}; \quad (6)$$

$$f_s = z_p \frac{n}{60}, \quad (7)$$

where z_p is the pole-pair number.

The electromagnetic torque expressed with the two-phase components is [1–3]:

$$m_e = K_{M1} z_p (\Psi_{sd\Theta} i_{sq\Theta} - \Psi_{sq\Theta} i_{sd\Theta}), \quad (8.1)$$

If the ARF components are substituted in the function of the current components, then there are put in evidence the two synchronous torques of different provenience, attributable to the PM and the variable reluctance:

$$m_e = K_{M1} z_p (\Psi_{PM} i_{sq\Theta} + 2\Delta L\, i_{sd\Theta} i_{sq\Theta}); \quad (8.2)$$

where the torque coefficient is K_{M1}= 3/2, if the variables correspond to amplitude of the instantaneous values.

The difference $2\Delta L = L_{sd} - L_{sq}$ expresses the effect of the variable reluctance. Its value in conventional machines is positive, but on the other hand many of the recently produced motors have negative reluctance torque which diminishes the main torque produced by the PM.

2.2. Steady state mathematical model of the PM synchronous motors

In electromagnetic steady state (StSt), when the current and the flux amplitude are constant, from the voltage equations (1) the derivative of the flux is eliminated, consequently the voltage equations are simplified, but the flux equations are not changed. These equations with two-phase components are:

– the armature voltage

$$\begin{cases} u_{sd\theta} = R_s i_{sd\theta} - \omega\Psi_{sq\theta}; \\ u_{sq\theta} = R_s i_{sq\theta} + \omega\Psi_{sd\theta}; \end{cases} \quad (9)$$

– the armature resultant flux

$$\begin{cases} \Psi_{sd\theta} = \Psi_{ssd\theta} + \Psi_{PM}; \\ \Psi_{sq\theta} = \Psi_{ssq\theta}; \end{cases} \quad (10)$$

– the armature reaction flux

$$\begin{cases}\Psi_{ssd\theta} = L_{sd} i_{sd\theta};\\ \Psi_{ssq\theta} = L_{sq} i_{sq\theta}.\end{cases} \quad (11)$$

In electromechanic StSt, when the speed is also constant, in the motion equation (5), the derivative of the speed results zero and the torque equation become:

$$m_e = m_L, \quad (12)$$

where the EMT results from (8.1) or (8.2).

In **Figure 2** is presented a version of the general StSt simulation structure created based on the (6) - (12) equations.

This variant is useful for checking the rated data (operation point) of the motor. Depending on the purpose of the modelling, there various simulation structures may be developed by swapping between one or more inputs and outputs.

Usually, the sinusoidal operation is calculated with RMS (*Root Mean Square*) values. In this case in expressions (8.1) and (8.2) the torque coefficient is $K_{M1} = 3$ **[1, 3]**.

3. The rated data of the PMSyM

The type of the motor is SIMOTICS S-1FL6/ Siemens AG (DE-97616 Bad Neustadt) **[7]**.

The motor rated data written on the name plate are:

– shaft torque $M_{tN} = 0.64$ Nm;
– shaft power $P_{tN} = 200$ W;
– revolutions per minute $n_N = 3000$ RPM;
– line current rms value $I_{vN}^{ef} = I_{sN}^{ef} = 1.4$ A (it is equal to the phase current).

Additional data from the motor manual:

– line voltage rms value $U_{vN}^{ef} = \sqrt{3}\, U_{sN}^{ef} = 111$ V, consequently the phase voltage $U_{sN}^{ef} = 64$ V;
– the rotor moment of inertia $J_r = 0.214\ 10^{-4}$ kg m^2;
– the load moment of inertia may be maximum 30 times the J_r **[7]**.

Measured parameters:

– armature resistance $R_s = 5.33\ \Omega$;
– longitudinal inductance $L_{sd} = 10.19$ mH;
– quadrature inductance $L_{sq} = 11.17$ mH;
– pole-pair number $z_p = 4$.

Calculated rated data:

– $f_{sN} = 200$ Hz, supply frequency;
– $M_{eN} = 0.731$ Nm, electromagnetic torque (EMT);
– $\cos\varphi_N = 0.95$ power factor;
– efficiency $\eta_N = 77.5\%$;
– $\Psi_{PM}^{Max} = 0.0615$ Wb, magnitude of the identified PM flux.

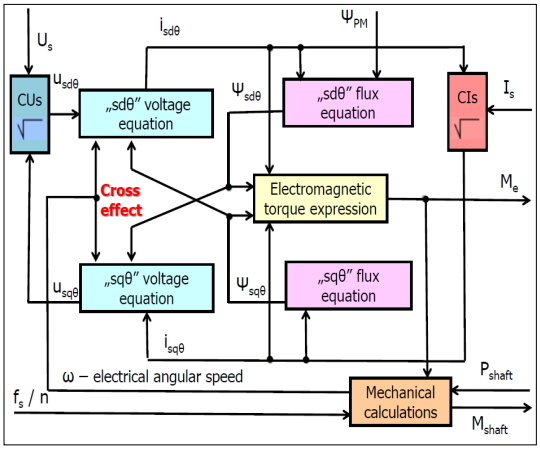

Fig. 2. *The general steady state simulation structure of the PMSyM.*

The measured parameters and the calculated data can be checked with the St_SimS from **Figure 2** for the rated operation point for the input rated values (voltage, current and frequency).

4. The control principle with the current vector perpendicular to the PM flux (CVpPMF)

The PMSyM-s with sinusoidal DMF have four fundamental control procedures **[4–6]**.

According to the best-known and most applied control principle the space phasor of the armature current is constrained to be perpendicular to the rotor longitudinal (direct) magnetic axis, i.e. to the PM-flux vector. In this case the two-phase components of the current space phasor have particular values: the direct component is zero, and the quadrature one is equal to the module of the current vector:

$$\begin{cases} i_{sd\theta} = 0;\\ i_{sq\theta} = i_s. \end{cases} \quad (13)$$

Based on (13) the longitudinal armature reaction (ArRe) flux $\Psi_{ssd\theta}$ is also zero. In this situation the resultant armature flux cannot be controlled to a constant value because the quadrature ArRe flux $\Psi_{ssq\theta}$ depends on the current and is determined by the mechanical load. Another disadvantage is the inductive character of the current because the motor with CVpPMF cannot operate at unity power factor. However, it has the advantage that the electromagnetic torque is produced with the minimum current value. On the other hand, for some new types of variable reluctance PM motors, with

$L_{sd} < L_{sq}$ (valid also for the above presented Siemens motor), the negative reluctance torque, that diminishes the PM torque, is cancelled due to the absence of the longitudinal ArRe flux.

4.1. Steady state phasor diagram with the CVpPMF

In **Figure 3** is presented the phasor diagram of the motor operating in steady state with the CVpPMF based on equations (9) - (11). This phasor diagram is valid for space phasors and at the same time for time phasors. It is also valid if the speed is variable in electromagnetic steady state, when the rms value of the current and fluxes is constant, because the diagram is independent of the variation of the speed in braking or acceleration operation of the motor.

4.2. Mathematical models with the CVpPMF

Considering the (13) condition, if the current vector ideally can be kept permanently perpendicular to the PM flux, in both dynamic and steady state operation, it leads to the simplified mathematical model of the PMSyM. Thus, the simplified simulation structures of the vector controlled PMSyM can be synthesized.

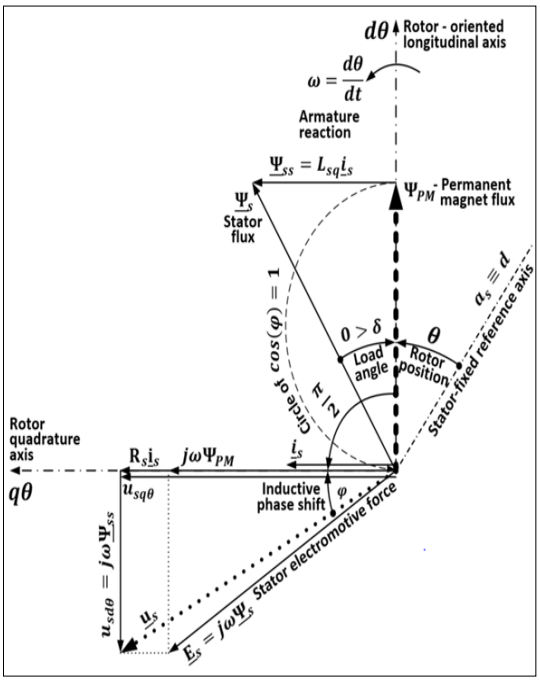

Fig. 3. *Electromagnetic steady state phasor diagram with the CVpPMF in dθ - qθ rotor-oriented synchronous rotating coordinate system.*

4.2.1. Steady state simplified mathematical model with the CVpPMF

Considering (13) and based on the (8) - (11) StSt equations, the simplified voltage, flux and torque expressions are the followings:

$$\begin{cases} \Psi_{ssd\theta} = 0; \\ \Psi_{ssq\theta} = \Psi_{ss} = L_{sq} i_s; \end{cases} \quad (14)$$

$$\begin{cases} \Psi_{sd\theta} = \Psi_{PM}; \\ \Psi_{sq\theta} = \Psi_{ssq\theta}; \end{cases} \quad (15)$$

$$\begin{cases} u_{sd\theta} = -\omega L_{sq} i_s; \\ u_{sq\theta} = R_s i_s + \omega \Psi_{PM}; \end{cases} \quad (16)$$

$$m_e = K_{M1} z_p \Psi_{PM} i_s, \quad (17)$$

and to these above (12) must be added, too.

4.2.2. Dynamic state simplified mathematical model with the CVpPMF

Considering (13) and based on the (1) - (8) general dynamic equations written with two-phase components, the simplified dynamic model results as follows:

$$\begin{cases} u_{sd\theta} = -\omega \Psi_{ss} = -\omega L_{sq} i_s; \\ u_{sq\theta} = R_s i_s + \omega \Psi_{PM} + L_{sq} \dfrac{di_s}{dt}, \end{cases} \quad (18)$$

and to these above the (5) motion equation, the (17) electromagnetic torque, and the (14) and (15) flux expressions must be added. In (18) the terms containing ω are the rotational electro-motive force (EMF) two-phase components while the term containg the current derivative is the self inducion voltage.

5. Vector controlled structures of the PMSyM drive

Based on the above presented MaMo-s there result the simplified simulation structures of the PMSyM drives. According to (5) and (12) the load torque contains the sum of all friction torques between the rotor and the load.

5.1. Simplified simulation structures without controllers

Modelling a simulation structure of the motor together with the whole control system, may result in more errors. In order to avoid that in the first step it is recommended to use simplified simulation structures without controllers considering ideally the perpendicularity of the current vector to the PM flux, based on the MaMo-s in steady state and dynamic operation modes presented in subsection 4.2.

5.1.1. Simplified static simulation structures (St_SimS) in steady state

According to the MaMo presented in paragraph 4.2.1 there is the possibility to create two different St_SimS-s depending on the input variables which beside the load torque may be the voltage or the frequency. The two St_SimS-s are presented in Figures 4 and 5, respectively. The structure with frequency (St_SimS_f) input is presented in Figure 4 where the voltage is the output.

In Figure 5 the presented simulation structure (St_SimS_U) has voltage and torque inputs and current and frequency outputs, respectively.

The similarity of both St_SimS-s consists in the load torque (equal to the EMT) input and the armature current output, which is proportional with the torque likewise the physical phenomena in the motor. In the structure St_SimS-s in steady state the calculations usually are made with rms values and in this case the torque coefficient $K_M = 3$, as it is written in Figures 4 and 5.

5.1.2. Simplified dynamic simulation structures (Dy_SimS)

There are two different Dy_SimS-s similarly to the previous subsection. These are based on the MaMo from paragraph 4.2.2 and differ in input, that is the voltage or the frequency beside the load torque. These St_SimS-s are presented in Figure 6 and 7, respectively.

The Dy_SimS-s contain only two derivatives, of the speed and of the armature current, the last one being equal with the torque producing (active) current component.

Due to the fact that in the Dy_SimS_U structure the voltage is the input, it contains integration blocks, as usually in the motor type MaMo-s. In the Dy_SimS_f structure, where the frequency is the input, instead of integration there appear derivative blocks and the voltage is an output, as in the case of generative type MaMo-s.

In the dynamic simulation structures the calculations usually are made with the amplitude of the variables, as in the classical Park models, consequently the torque coefficient $K_M = 3/2$, as it is written in Figure 6 and 7.

5.2. Simulation structures with controllers

The vector control structure which is suitable for implementation is presented in Figure 8, where the perpendicularity of the current vector to the PM flux is provided by means of cancelling the longitudinal ArRe, according to (13) controlling the current component $i_{sd\theta}$ to zero value. Besides that the speed is controlled by a cascade control structure by means of the active quadrature current component $i_{sq\theta}$, which in steady state is equal to the modulus of the i_s armature current.

The actuator is a carrier-wave controlled pulse-width modulated (PWM) voltage-source

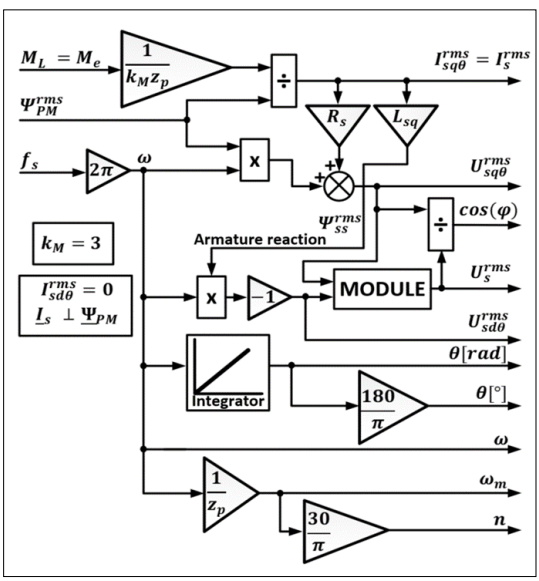

Fig. 4. *Static simulation structure (St_SimS_f) block diagram of the PMSyM with the CVpPMF with frequency and torque inputs, and current and voltage outputs, respectively* [8].

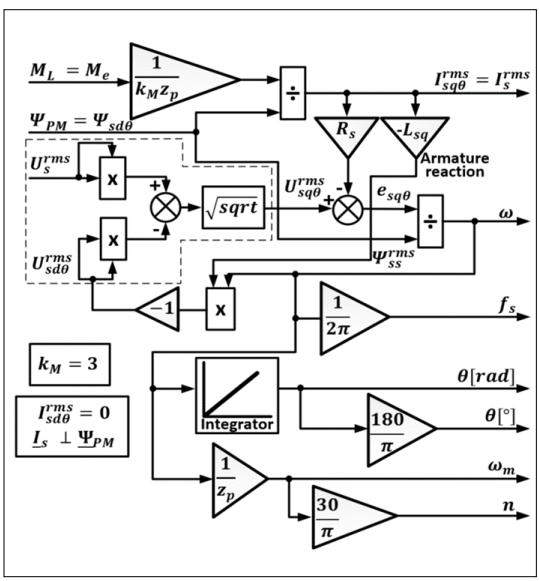

Fig. 5. *Static simulation structure (St_SimS_U) block diagram of the PMSyM with the CVpPMF, with voltage and torque inputs and current and frequency outputs, respectively.*

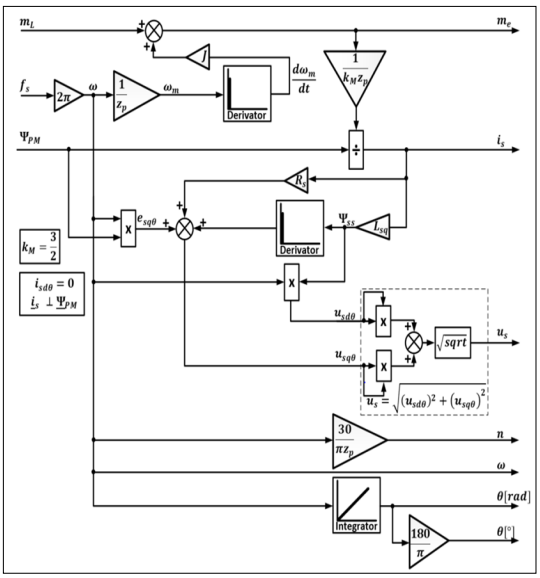

Fig. 6. *Dynamic simulation structure (Dy_SimS_f) block diagram of the PMSyM with the CVpPMF with frequency and torque inputs and current and voltage outputs, respectively.*

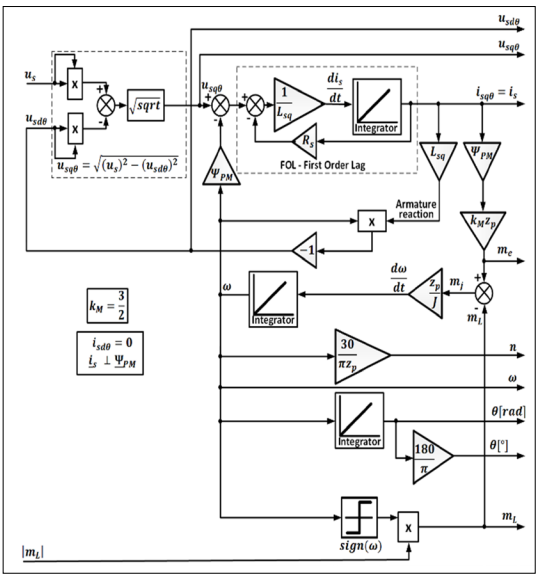

Fig. 7. *Dynamic simulation structure (Dy_SimS_U) block diagram of the PMSyM with the CVpPMF with voltage and torque inputs and current and frequency outputs, respectively* **[8]**.

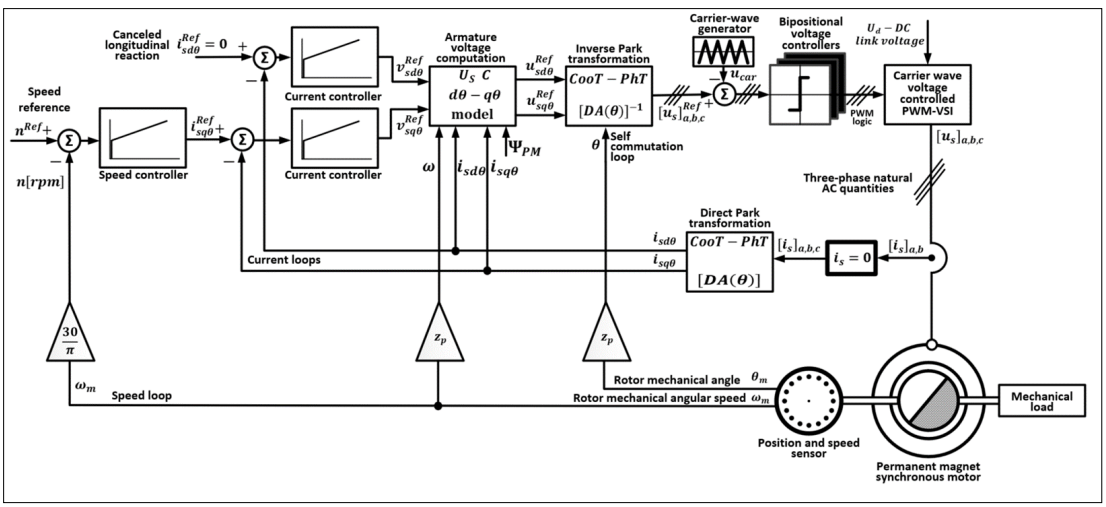

Fig. 8. *Vector control structure of the synchronous motor drive fed by carrier wave PWM controlled voltage-source inverter (VSI) with the current vector perpendicular to the PM flux.*

inverter (VSI), which practically is a three-phase IGBT bridge DC-AC converter. The two-phase components of the armature current are imposed as reference values. The active component reference value is generated by the speed controller. Because the PWM procedure is of voltage-controlled type, it needs voltage references. That is why the U_sC block is needed, which is compiled upon the PMSyM MaMo, as follows:

$$\begin{cases} u_{sd\theta}^{Ref} = v_{sd\theta}^{Ref} - \omega L_{sq} i_{sq\theta}; \\ u_{sq\theta}^{Ref} = v_{sq\theta}^{Ref} + \omega L_{sd} i_{sd\theta} + \omega \Psi_{PM}, \end{cases} \tag{19}$$

where the speed ω and the current components result as feedback.

The two control variables generated by the current controllers are determined based on the scalar equations derived from (1), as follows:

$$\begin{cases} v_{sd\theta}^{Ref} = R_s i_{sq\theta} + L_{sd} \dfrac{di_{sd\theta}}{dt}; \\ v_{sq\theta}^{Ref} = R_s i_{sq\theta} + L_{sq} \dfrac{di_{sq\theta}}{dt}. \end{cases} \quad (20)$$

In this vector control structure, the PMSyM is simulated using the MATLAB-Simulink® library model of the 3-phase motor, whith the MaMo presented in **Figure 9**.

The internal PMSM block is based on (1) - (8) general equations written with rotor-oriented, i.e. PM-field-oriented two-phase components. It is connected to the external three-phase system (inverter and PWM control unit) with the direct and reverse Park transformation blocks (CooT-PhT). In fact the Park-transformation is composed of two elementary transformations, the so-called „3/2" Clarke phase transformation (PhT) and the conventional coordinate transformation (CooT).

The matrix operator of the Park-transformation results by combining the two elementary matrix operators and it results:

$$[DA(\theta)] = \\ = \frac{2}{3}\begin{bmatrix} \cos(\theta) & \cos\left(\theta - \frac{2\pi}{3}\right) & \cos\left(\theta + \frac{2\pi}{3}\right) \\ -\sin(\theta) & -\sin\left(\theta - \frac{2\pi}{3}\right) & -\sin\left(\theta + \frac{2\pi}{3}\right) \\ \frac{1}{2} & \frac{1}{2} & \frac{1}{2} \end{bmatrix}. \quad (21)$$

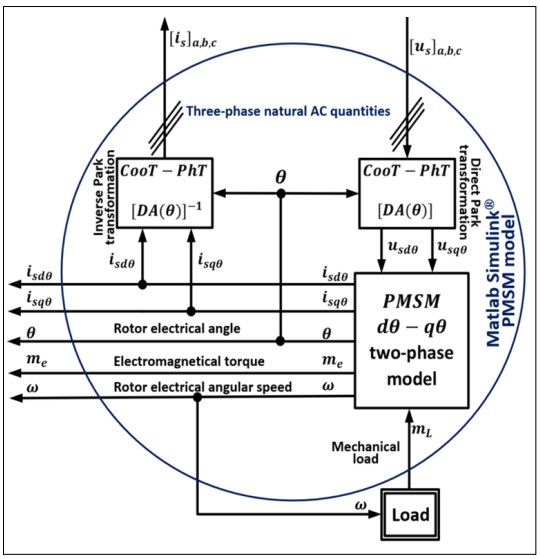

Fig. 9. *Block diagram of the three-phase motor model from the MATLAB-Simulink® library.*

Whith the $[DA(\theta)]$ operator the direct Park-transformation can be written as follows:

$$\begin{bmatrix} g_{sd\theta} \\ g_{sq\theta} \\ g_{s0} \end{bmatrix} = [DA(\theta)] \begin{bmatrix} g_{sa} \\ g_{sb} \\ g_{sc} \end{bmatrix}, \quad (22)$$

where the variable g may be current (i), voltage (u, v, e, Δu), or flux (Ψ), etc **[1–3]**.

The matrix operator of the reverse Park-transformation is:

$$[DA(\theta)]^{-1} = \\ = \begin{bmatrix} \cos(\theta) & -\sin(\theta) & 1 \\ \cos\left(\theta - \frac{2\pi}{3}\right) & -\sin\left(\theta - \frac{2\pi}{3}\right) & 1 \\ \cos\left(\theta + \frac{2\pi}{3}\right) & -\sin\left(\theta + \frac{2\pi}{3}\right) & 1 \end{bmatrix}. \quad (23)$$

With this matrix the reverse Park-transformation is written as below:

$$\begin{bmatrix} g_{sa} \\ g_{sb} \\ g_{sc} \end{bmatrix} = [DA(\theta)]^{-1} \begin{bmatrix} g_{sd\theta} \\ g_{sq\theta} \\ g_{s0} \end{bmatrix}. \quad (24)$$

The reverse Park-transformation is applied in **Figure 9** inside the motor block for the output currents and in **Figure 8** in the control structure for the voltage references, corresponding to a three-phase sine-wave vectorial signal generator.

The direct Park-transformation is applied in **Figure 8** in the control structure for the feedback currents and in **Figure 9** inside the motor block for the input voltages.

Because in the MaMo of the motor block the current two-phase components are state variables, these can be directly connected to the input of the UsC voltage computation block, consequently the direct Park-transformation is not needed to provide the current feedback in the simulation of the control structure from **Figure 8**, only for its implementation, however, it is necessary to generate the voltage reference values by means of a reverse Park-transformation.

For the compatiblity between the simulation results of the vector control structure from **Figure 8** the motor calculations and the simulation results of the simplified structures, which are applied for sinusoidal operation, the control structure will be simulated with sine-wave variables, without PWM-control of the VSI.

6. Simulation results

The simulations were gradually performed, starting with the simplest static structures, compared with the dynamic ones, in which the per-

pendicularity of the current to the PM flux was realized without controllers. So, we can check the motor measured parameters and the calculated rated data. It was only after these initial steps that we simulated the drive control system with the structure shown in **Figure 8.**

In simulations of the vector control structures the moment of inertia value J_{Eq} = 5.5 10^{-4} kgm^2, was similar to the simulations of the simplified dynamic structures (Dy-SimS). The value of the moment of inertia does not exceed the permissible limit given in the motor manual, which in our case is J_{Eq}^{Max} = 6.634 10^{-4} kgm^2.

6.1. Simplified simulation structures with voltage input

The simulation results of the simplified static (St_SimS_U) and dynamic (Dy_SimS_U) structures with voltage and load torque input are presented in **Figures 10–12.**

In **Figure 10** can be seen that the voltage was is linearly increased from the

$$U_{s0}=\Delta u_R=R_s I_{sN}^{ef}=5.33\Omega\ 1.4\text{A}=7.462\ \text{V}$$

boost value, and the torque from zero to the rated value in 1 s, and held at these values for 1 s, while the system reached the steady state and both the current and the speed (frequency) reached their rated values. Then in 1 s maintaining the torque at rated value, the motor voltage was reduced to the U_{s0} boost value, which corresponds to the steady state at zero speed and rated load torque.

Figure 10 shows the speed as a function of torque, according to the cycle described above for both simplified structures, i.e. the static (St_SimS_U) and dynamic (Dy_SimS_U) ones. The intersection of the two mechanical characteristics (MeCh) is clearly visible during both steady states, at rated load torque and rated or zero speed, respectively.

In the time diagrams from **Figures 11** and **12** in steady state, during the 1 – 2 s and 3 – 4 s intervals, the corresponding variables become equal, i.e. the static and dynamic curves are superimposed.

The transients of the current and of the EMT proportional to the current can be attributed to the lack of voltage control, despite of ramping of the voltage and load torque inputs instead of step variation, both during starting and braking.

A completely different result is obtained with the frequency input structures, where the calculation of the voltage would correspond to an ideal voltage control.

6.2. Simplified simulation structures with frequency input

The simulation results of the simplified static (St_SimS_f) and dynamic (Dy_SimS_f) structures with frequency and load torque input are presented in **Figures 13–15**, where the RPM value is represented instead of the frequency ($n = 60\, f_s/z_p$).

The acceleration during starting and the deceleration at braking take place under constant dynamic torque, when due to the linearly increasing load the current also increases linearly.

In the simulation results of the frequency input dynamic structure spikes appear caused by the signal derivatives, which in the saved results are detected and filtered with the „ischange" (*„in_array"*, *„MaxNumChanges"*, *„maxChanges"* parameter) MATLAB® function.

Compared to the results of the previous subsection obtained in the case of the voltage input structure, where decaying transients appear due to the first order lag (FOL), in case of the frequency input structure the transients disappear instantaneously without any delay.

6.3. Vector control structure with sinewave variables without PWM

The ideal sinusoidal operation of the vector control simulation structure (VC_SimS_Sin) is solved by omitting in **Figure 8** the PWM-VSI and the three-phase supply of the motor MaMo from **Figure 9** is simulated with the three modulation reference signals $[u_s]_{a,b,c}^{Ref}$. The simulation results of the above-described VC_SimS_Sin structure are shown in **Figures 16–18** and **22.**

The simulation was performed under the same conditions as for the simplified structures, according to the same load cycle. The reference signal of the speed was also increased for starting and reduced at braking with a ramp function in the same manner as for the static structure.

By simulating the VC_SimS_Sin, the correctness of the Simulink® motor block parameterization can be checked, by comparing it with the previously simulated simplified structures, because in steady state the same results should be obtained regardless of which structure is involved.

6.4. Vector control structure of the PWM-voltage fed PMSyM

The vector-controlled drive system shown in **Figure 8** was simulated with the three-phase motor model from **Figure 9** (it is called VC_Sim_PWM)

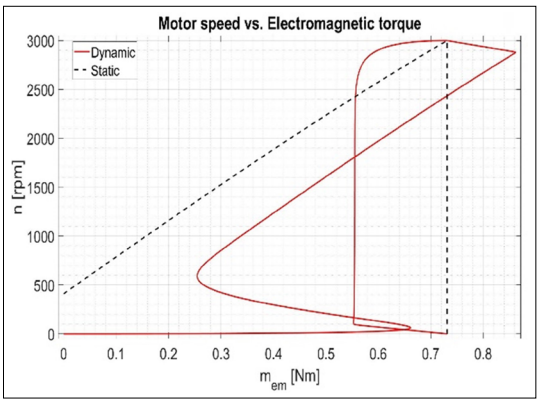

Fig. 10. *Static (black dashed) and dynamic (red) mechanical characteristics simulated with the voltage input structures from Fig. 5 (St_SimS_U) and Fig. 7 (Dy_SimS_U).*

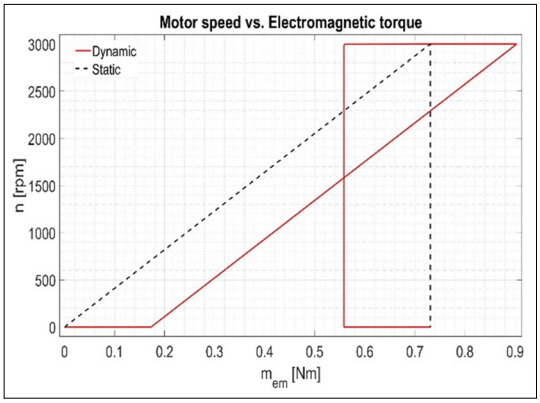

Fig. 13. *Static (black dashed) and dynamic (red) mechanical characteristics simulated with the frequency input structures from Fig. 4 (St_SimS_f) and Fig. 6 (Dy_SimS_f).*

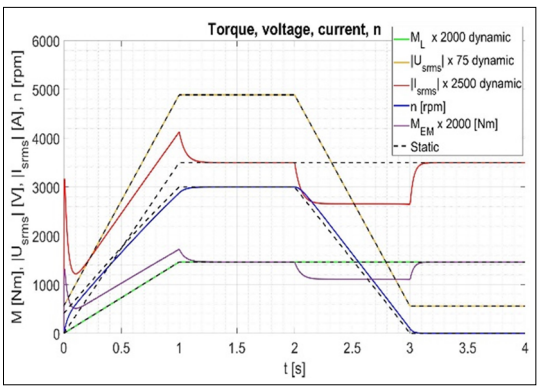

Fig. 11. *Static (black dashed) and dynamic (colored lines) time diagrams simulated with the structures from Fig. 5 (St_SimS_U) and Fig. 7 (Dy_SimS_U): input voltage (yellow) and load torque (green), the output current (red), speed (blue) and EM torque (purple).*

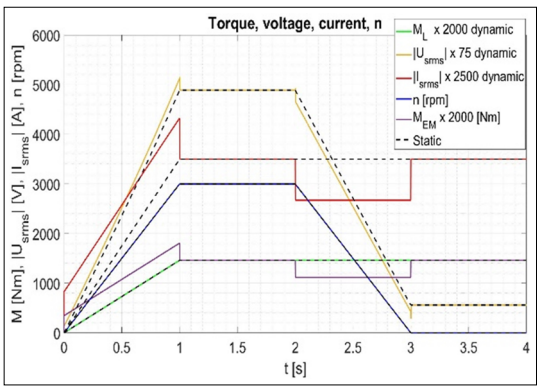

Fig. 14. *Static (black dashed) and dynamic (colored lines) time diagrams simulated with the structures from Fig. 4 (St_SimS_f) and Fig. 6 (Dy_SimS_f): input speed (blue) and load torque (green), the output voltage (yellow), current (red) and EMT (purple).*

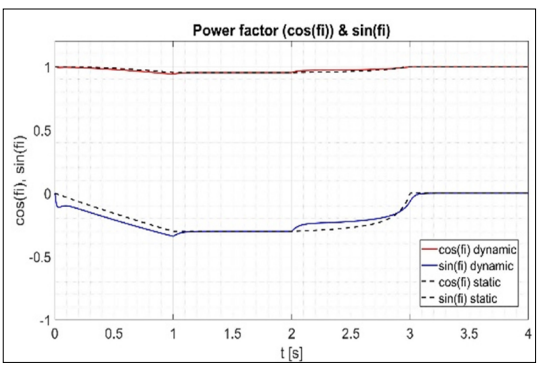

Fig. 12. *Static (black dashed) and dynamic (colored lines) time diagrams of the cosφ power factor (red) and sinφ (blue) simulated with voltage input structures.*

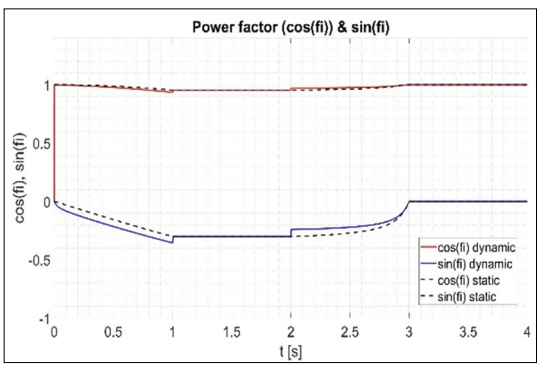

Fig. 15. *Static (black dashed) and dynamic (colored lines) time diagrams of the cosφ power factor (red) and sinφ (blue) simulated with frequency input structures.*

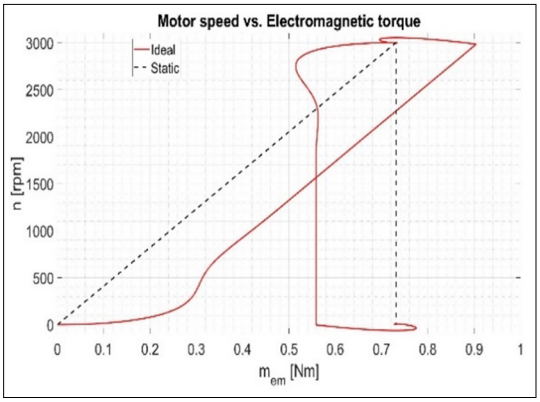

Fig. 16. *Static (black dashed) and dynamic (red) mechanical characteristics of the vector control structure (VC_SimS_Sin) simulated with the Simulink® motor block fed by sinusoidal voltages.*

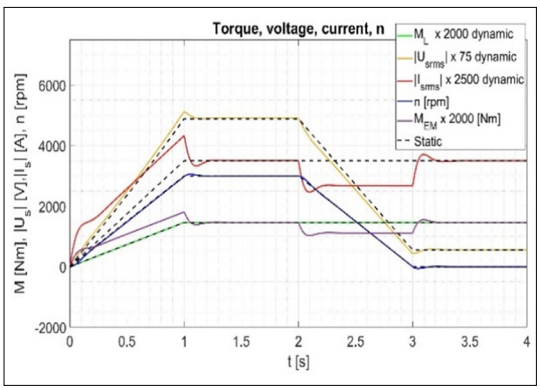

Fig. 17. *Static (black dashed) and dynamic (colored lines) time diagrams of the VC_SimS_Sin structure: load torque (green), EMT (purple), speed (blue), current (red) and voltage (yellow).*

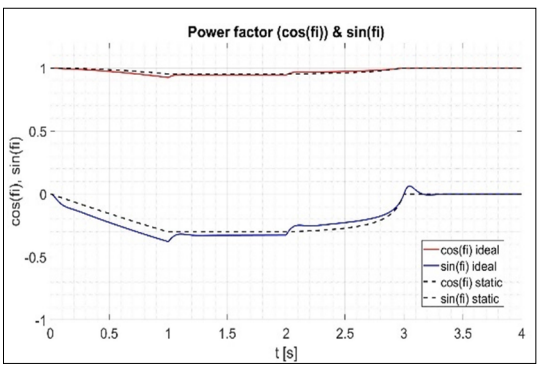

Fig. 18. *Static (black dashed) and dynamic (colored lines) time diagrams of the cosϕ power factor (red) and sinϕ (blue) simulated with the VC_SimS_Sin structure.*

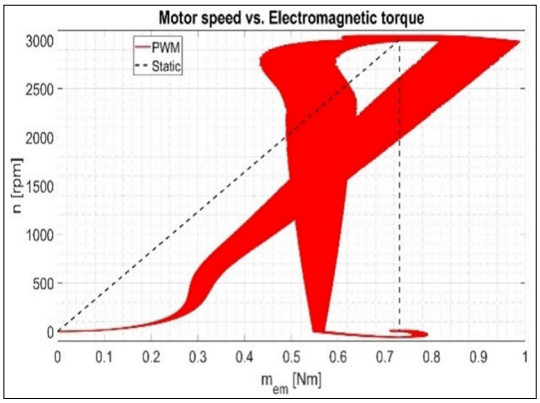

Fig. 19. *Static (black dashed) and dynamic (red) mechanical characteristics of the vector control structure (VC_SimS_PWM) simulated with the Simulink® motor block fed by an ideal PWM-inverter.*

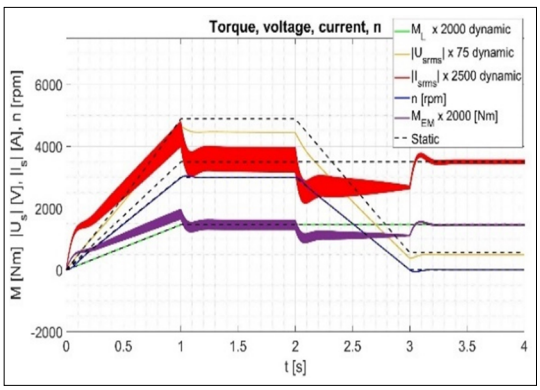

Fig. 20. *Static (black dashed) and dynamic (colored lines) time diagrams of the VC_SimS_PWM structure: load torque (green), EMT (purple), speed (blue), current (red) and voltage (yellow).*

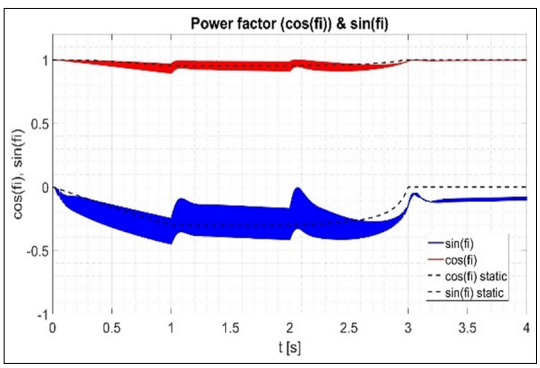

Fig. 21. *Static (black dashed) and dynamic (colored lines) time diagrams of the cosϕ power factor (red) and sinϕ (blue) simulated with the VC_SimS_PWM structure.*

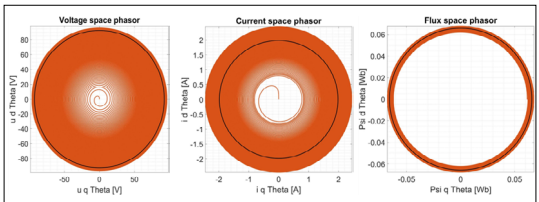

a) Armature voltage b) Armature current c) Resultant flux

Fig. 22. *Space-phasor diagrams of the structure VC_SimS_Sin during the first 1.5 seconds of the start-up (orange) and in rated steady state during ten periods in 1.45 - 1.5 s interval (black).*

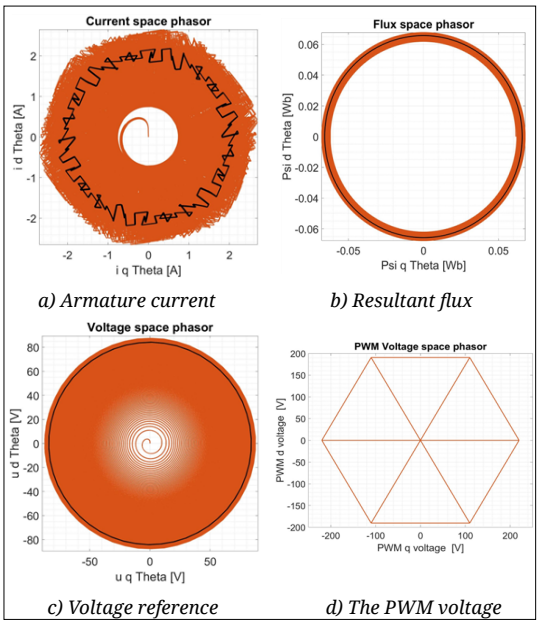

a) Armature current *b) Resultant flux*

c) Voltage reference *d) The PWM voltage*

Fig. 23. *Space-phasor diagrams of the structure VC_SimS_PWM during first 1.5 seconds start-up (orange) and in rated steady state during ten periods in 1.45 - 1.5 s interval (black).*

under the same conditions as the previous structures, with the difference that there was included an idealized PWM-inverter model realized with simple bi-positional switches.

The three-phase motor block is connected to the output of the ideal inverter by the „*Controlled Voltage Source*" Simulink® library block.

The simulation results obtained with 220 V DC link voltage and f_s^{CrW} = 5 kHz frequency of the carrier wave are shown in **Figures 19–21** and **23.**

The simulation results were generated with maximim integration step size: 5 µs by means of the solver method „ode23t(mod.Stiff/Trapezoidal)".

Compared to the results of the subsection 6.3 the effect of the PWM control in pulsation of the current and electromagnetic torque EMT is clearly visible.

The effect of the PWM control also occurs in the input errors of the current component controllers, but it is no longer noticeable in the speed error, because the drive system naturally filters it out thanks to the moment of inertia of the drive.

The recommended minimum frequency of the carrier wave must be at least 20 times the maximum f_s stator frequency, which at the rated value f_{sN} = 200 Hz would be minimum f_{Min}^{CrW} = 4 kHz, so the modulation frequency used in the simulation meets this condition.

It is noticeable that at starting with increasing the operating frequency the pulsation of the current and electromagnetic torque increases. This can be explained by the fact that at low speeds, where the supply frequency is also low, the number of the modulated pulses during a period is higher than at the rated speed.

According to the procedure presented in this paper the experimentally determined parameters and calculated data of a given motor can be checked.

7. Conclusions

The simulation results of the two simplified static structures, with two types of input (St_SimS_U and St_SimS_f), are the same.

The steady state of the dynamic structures is the same, but the transient processes differ.

Furthermore, the correctness of the MaMo parameterization used in the simulations can also be checked.

The presented simulation results confirm the correct identification of the motor data and parameters and prove the functional ability of the vector control structure.

In the future, the motor feeding will be simulated with the „*Universal Bridge*" inverter model from the Simulink® library, which will be even closer to the practical solution.

In the following, in the vector control structure the carrier wave modulation will be replaced with space vector modulation (SVM), which can optimize the inverter operation with the so-called "flat top" two-phase modulation, reducing the commutation losses by up to 30%.

The research continues with the implementation of the vector control drive system on a test bench built in the power electronics laboratory in the Faculty of Târgu Mureş of the Sapientia Hungarian University of Transylvania.

References

[1] Kelemen A., Imecs M.: *Sisteme de reglare cu orientare după cîmp ale mașinilor de curent alternativ.* Editura Academiei Române, București, 1989.

[2] Kelemen Á., Imecs M.: *Vector Control of AC Drives.* Vol. 2: *Vector Control of Synchronous Machine Drives*. Écriture Kiadó, Budapest, 1993.

[3] Imecs M., Szabó Cs.: *Permanens-mágneses-forgórészű szinkronmotor. Terminológia, Magyar nyelvű szakelőadások a 2002–2003-as tanévben.* Erdélyi Magyar Műszaki Tudományos Társaság – EMT, Kolozsvár, 2004, 56–64.

[4] Imecs M., Birou I., Jánky P., Kelemen Á.: *High performance control of PM-synchronous servomotors using the MS320C5x processor*. Intelligent Motion, International Conference on Power Electronics and Intelligent Motion – PCIM'97, Nürnberg, Germany, 1997, 157–166.

[5] Imecs M.; Birou, I.; Szabó, Cs.: *Control strategies for synchronous motors with permanent magnet or constant exciting current.* Proceedings of Power Electronics and Intelligent Motion International Conference – PCIM'99, Nurnberg, Germany, June 22–24, 1999, 339–344.

[6] Imecs M., Birou I., Szabó Cs.: *Modelling and simulation of vector-control strategies for PM-synchronous motors.*, Proceedings of the IEEE-TTTC International Conference on Automation, Quality and Testing, Robotics Q&A-R 2000, Tome 2, Cluj-Napoca, 2000, 151–156.

[7] *** Product Details - Industry Mall - Siemens China, SIMOTICS S-1FL6 SERVO MOTOR Manual (add-furnace.com) https://www.add-furnace.com/product-catalog/siemens/simotics-s-1fl6-servo-motor-manual.pdf

[8] Imecs M., Ferencz J., Kelemen A.: *Vektoriálisan szabályozott permanens mágneses szinkron gépes hajtás egyszerűsített modellezése és szimulálása.* ENELKO 2023 – XXIV. Nemzetközi Energetika-Elektrotechnika Konferencia, Kolozsvár, 2023. okt. 12–15, EMT, Kolozsvár, 2023.10.11, 7–13. https://ojs.emt.ro/enelko-szamokt/issue/view/59 https://ojs.emt.ro/enelko-szamokt/article/view/1340/1350

[9] IEC/EN 60034-30-1, International Efficiency Classes, Standard on Efficiency Classes for Low Voltage AC Motors. https://webstore.iec.ch/publication/136